

1
2 **THERMAL PROPERTIES OF ACACIA MANGIUM CROSS**
3 **LAMINATED TIMBER AND ITS GLUELINES BONDED WITH TWO**
4 **STRUCTURAL ADHESIVES**

5
6 **Norwahyuni Mohd Yusof ¹, Paridah Md Tahir ^{1*}, Lee Seng Hua ^{1*}, Fatimah Athiyah**
7 **Sabaruddin ¹, Redzuan Mohammad Suffian James ¹, Mohd Asim Khan ¹, Lee Ching**
8 **Hao ¹, Adlin Sabrina Muhammad Roseley ²**
9

10
11 ¹ Institute of Tropical Forestry and Forest Products, University Putra Malaysia, 43400 UPM
12 Serdang, Selangor Darul Ehsan, Malaysia.

13 ² Faculty of Forestry and Environment, University Putra Malaysia, 43400 UPM Serdang,
14 Selangor Darul Ehsan, Malaysia.

15
16 * **Corresponding authors:** parida@upm.edu.my; lee_seng@upm.edu.my

17 **Received:** October 21, 2019

18 **Accepted:** August 17, 2020

19 **Posted online:** August 17, 2020
20

21 **ABSTRACT**

22
23 The properties of CLT can be affected by the type of adhesives used. The thermal properties
24 of the adhesive that joins the timber together is essential to determine the thermal endurance
25 of the CLT product. In this study, two types of adhesives were used to join the cross
26 laminated timber (CLT) manufactured from *Acacia mangium* namely phenol resorcinol
27 formaldehyde (PRF) and one component polyurethane (PUR). The thermal properties of the
28 adhesives, *A. mangium* wood and the gluelines were determined via Thermogravimetric
29 Analysis (TGA) and Dynamic Mechanical Analysis (DMA) tests. The TGA test showed
30 that PRF adhesive had higher degradation temperature at 530 °C compared to PUR adhesive
31 at 430 °C. Meanwhile, the PRF adhesive as a glueline in CLT also showed better thermal
32 resistance where a higher amount of residue of 20,94 % was recorded at temperature up to
33 900 °C compared to PUR glueline with 18,26 % residue. The integrity of the CLT over
34 temperature were determined via DMA test and the results showed that PRF adhesive as
35 glueline had superior properties, indicating better interfacial bonding with the woods.

36
37 **Keywords:** *Acacia mangium*, dynamic mechanical analysis, one component polyurethane,
38 phenol resorcinol formaldehyde, thermogravimetric analysis.

INTRODUCTION

42
43
44
45
46
47
48
49
50
51
52
53
54
55
56
57
58
59
60
61
62
63
64
65

Cross-laminated timber (CLT) is a wood panel composite that joining at least three layers of solid-sawn timber by using adhesive (Sutton *et al.* 2011). This material has been considered as high demand products that used as a constructional material for buildings. It enables a rapid installation for wall and floor structure that suitable for most finishes (Van De Kuilen *et al.* 2011). According to Dieste *et al.* (2019), CLT is a highly value-added products compared to that of the other wood products. The mass production of CLT is formed in a similar way to “glue-laminated timber” beams using permanent adhesives which the limitations such as knots, checks, splits, warping and weathering can be removed to reduce variability and enhanced its structural properties. Almost all the studies of CLTs reported are constructed from softwood species such as spruce, larch, white fir, silver fir, Douglas fir, pine and yellow poplar with density ranging from 350 kg/m³ to 700 kg/m³ (Engineering Toolbox, 2004). For instance, Wang *et al.* (2018) fabricated CLT from spruce-pine-fir lumber pieces to study the effects of edge-gluing and gap size in the cross layers.

The rapid industrialization and increasing number of populations in the world causes depleting of forest wealth at a rapid rate. The issue has urged the manufacturers to make use of fast grown plantation species for various timber applications (Shukla 2019). To relieve the pressure of the continuous extraction of logs from local natural forest, the establishment of plantation forests is a matter of utmost urgency. In 2005, a Forest Plantation Programme has been implemented by Ministry of Plantation Industries and Commodities (MPIC) where a total of 375000 ha of forest plantation has been targeted to be developed at the end of 2020. The programme aims to ensure the sustainability of the raw materials supply for the domestic

66 timber industry. *Acacia* spp. (*mangium* /hybrid) and rubberwood (Timber Latex Clone) are
67 the two major species out of nine selected species under this programme.

68

69 *A. mangium* is one of the fast-growing and sustainable species for potentials timber
70 production. It has a wood density ranging from 420 kg/m³ to 483 kg/m³ for green soaked
71 volume and 500 kg/m³ to 600 kg/m³ in dry condition (Kasim *et al.* 2014). In another study,
72 the density of *A. mangium* was reported to fall within a range of 290 kg/m³ to 675 kg/m³. The
73 density increases as the age of tree increased from 2 years to 20 years (Nordahlia *et al.* 2013).
74 The density of wood is the best method to determine the quality of wood and correlated to its
75 product's strength and shrinkage (Nugroho *et al.* 2012; Miranda *et al.* 2007; Lim *et al.* 2003).
76 Wood is a renewable material and it has many applications. However, wood is easily
77 degraded by sunlight, moisture and temperature due to the organic structure and the most
78 important challenges of the components of wood is thermal decomposition of cellulose,
79 lignin and hemicellulose at the low temperature (100 °C to 150°C) (Aydemir *et al.* 2016).
80 Hence, wood have different degradation points and is highly dependent on their specific
81 chemical compositions.

82

83 The selection of the adhesives to manufacture the CLT is very important as it needs to
84 meet the characteristics and the application of the CLT itself. Polyurethane (PUR) adhesive
85 glue is well known as a formaldehyde-free adhesive for exterior grade structure application
86 for GLULAM and finger-joint in several European countries (Richter *et al.* 2006). Other than
87 that, the thermal properties of the CLT are also very important but there is very limited
88 information on this topic been reported. According to Asim *et al.* (2018), excellent thermal
89 and fire-retardant behaviour of phenol resorcinol formaldehyde (PRF) adhesive glue allowed

90 it to be used in building structural materials and automobile industry. Some studies have been
91 conducted to compare the performance of PRF and PUR adhesives in CLT fabrication.
92 Norwahyuni *et al.* (2019a) compared both PRF and PUR adhesive in bonding CLT from *A.*
93 *mangium* wood. The authors reported that PRF adhesive performed better than that of PUR
94 adhesive as it led to higher shear bond strength and wood failure percentage. In another study,
95 Norwahyuni *et al.* (2019b) evaluated the mechanical and physical properties of *A. mangium*
96 CLT bonded with PRF and PUR. The results revealed that the CLT bonded with PRF
97 adhesive exhibited higher mechanical properties compared to that of the PUR-bonded CLT.
98 Nevertheless, information on the thermal stability of PRF and PUR in CLT manufacturing
99 are rather limited.

100

101 Therefore, the objective of this study is to evaluate the thermal properties of neat PRF
102 and PUR adhesive, *A. mangium* wood as well as the glueline formed between wood and
103 adhesive. The glueline formed between two adjacent layers of wood is important as it might
104 impart some thermal resistance to the wood itself. Through the thermal studies, the thermal
105 degradation, weight loss, final residue, decomposition temperature of each component
106 samples was assessed based on peak DTG curves, storage modulus, loss modulus and
107 damping factor of the samples.

108

109

110

MATERIALS AND METHODS

111

Manufacturing Cross Laminated Timber (CLT) species

112

113

114

115

Twenty-year-old *A. mangium* wood with a density of 673 kg/m³ and moisture content of
12 % ± 3 % was obtained from a local lumber mill located at Bukit Rambai, Melaka,

116 Malaysia. The wood was sawn, trimmed and planed into 1000 mm long by 70 mm wide and
117 18,2 mm thick lumber. In this study, a 3-layer CLT of 1000 mm × 280 mm × 54,5 mm in size
118 was produced by glueing three pieces of lumbers parallel and perpendicular to each other
119 with edge bonding with 90° alternating transverse CLT layers. Boards were glued using two
120 types of adhesive, namely phenol resorcinol formaldehyde (PRF) and one component
121 polyurethane (PUR). Both types of adhesives were applied to the samples at a spreading rate
122 of 250 g/m² within a short time to avoid possible oxidation and dimensional instability. The
123 assemblies were then subjected to a pressure of 1,5 N/mm² at 30 °C for 90 minutes using a
124 compressive machine. In the next stage, the laminated panels were conditioned at 65 % ± 5
125 % RH and 20 °C ± 2 °C for 2 weeks before cutting them into specimens for properties
126 evaluation. Two types of adhesives were used in this study i.e., phenol resorcinol
127 formaldehyde (PRF 1734 AkzoNobel) and one component polyurethane (1C-PUR or PUR,
128 Jowapur 687,22). Hardener 2734 (commercial code) was also used in the preparation of PRF
129 at a ratio of 100 to 25 parts by weight of PRF to hardener.

130 **Characterization of the samples**

131

132 **Thermogravimetric Analysis (TGA)**

133

134 Thermal stability of both PRF and PUR adhesives, *A. mangium* wood and glue line
135 formed between wood and adhesives after pressing were characterized using
136 Thermogravimetric analyser (TGA Q 500 TA Instrument, USA) at Institute of Tropical
137 Forestry and Forest Product (INTROP), Universiti Putra Malaysia (UPM). In order to
138 eliminate the effect of initial mass, 10 mg of sample was used for each experiment and placed
139 in an alumina crucible. Non-isothermal TGA was conducted with the temperature raised from
140 10 °C to 900 °C with a rate of 10 °C/min in an oxygen atmosphere. The gas was purged at a
141 constant flow rate of 30 mL/min. Three replications were used for every adhesive type tested.

142 A total of 15 specimens (3 x [PRF and PUR adhesives + *A. mangium* wood + glueline formed
143 by both adhesives]) were tested in this study.

144

145 **Dynamic mechanical analysis (DMA)**

146

147 Dynamic mechanical analysis (DMA) was executed to determine the viscoelastic
148 behaviour of specimens from 30 °C to 150 °C with a heating rate of 5 °C/min and controlled
149 sinusoidal strain. DMA test was performed by employing TA (DMA Q 800) instrument at
150 INTROP, Universiti Putra Malaysia, and operating in a three-point bending mode with 1 Hz
151 oscillation frequency under controlled amplitude. The specimens having dimensions of 60
152 mm × 12 mm × 6 mm (l × w × t) were used for the testing. For DMA, only PRF and PUR
153 gluelines were tested with three replications each. Therefore, a total of 6 specimens were
154 evaluated.

155

156

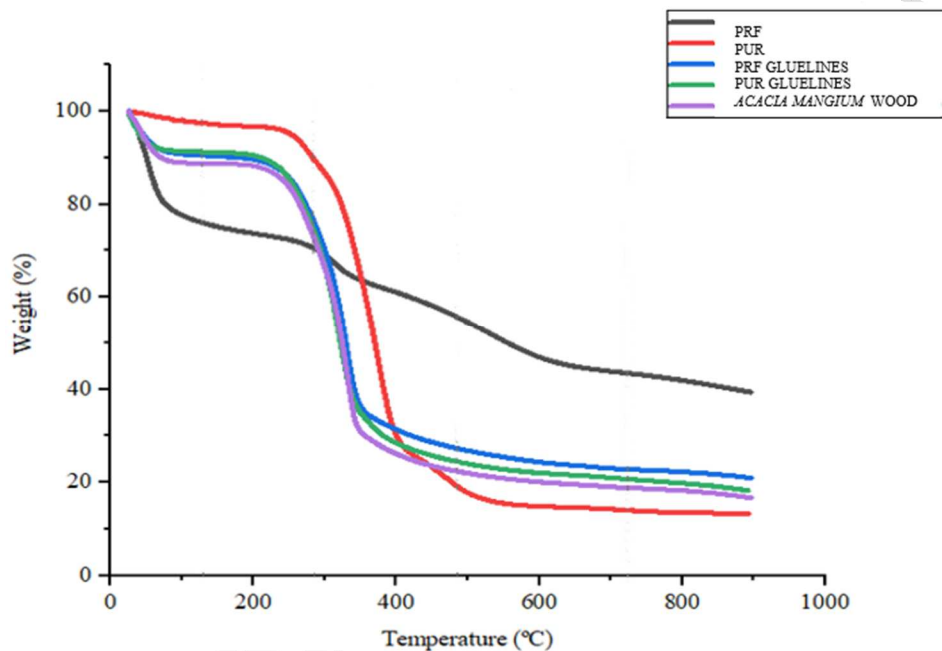
156 **RESULTS AND DISCUSSION**

157

158 **Thermogravimetric Analysis (TGA)**

159

160 Heat resistance of a material is one of the most important criteria's in any building
161 construction. Since wood is combustible, the application of wood as building material becomes
162 very limited. Thus, thermal evaluation is an essential method to determine the capability of the
163 material to resist heat. In general, TGA is used to observe the material's thermal stability and
164 degradation behaviour. TGA analysis on the neat adhesive (PRF and PUR), glueline between
165 wood and the adhesive and *A. mangium* wood are demonstrated in Figure 1 and Table 1.



166 **Figure 1:** TGA curve of PRF, PUR, PRF glueline, PUR glueline and *A. mangium* wood.
167

168 During thermal degradation, drying of free water and major mass loss due to devolatilization
169 and thermal debonding has been observed. All samples experienced a slight weight loss at
170 temperature below 100 °C as shown in Figure 1 due to evaporation or dehydration of the water
171 molecules (Sanyang *et al.* 2015; Nadirah *et al.* 2012; Johar *et al.* 2012). Significant weight loss
172 (26,8 %) was observed for PRF adhesive glue at a temperature less than 100 °C due to the high
173 amount of volatile free formaldehyde and phenol other than free water removal. This finding was
174 aligned with the findings from previous studies done by Asim *et al.* (2018) and Liu *et al.* (2017).
175 Both adhesives showed similar initial degradation temperature which occurred at 220 °C.

176 However, PUR adhesive showed a higher weight loss of 74,40 % compared to PRF adhesive
 177 with the amount of weight loss of 47,92 % during the main degradation process. This finding
 178 could be attributed to the availability of the thermally unstable urethane bond in PUR adhesive
 179 that leads to rapid degradation (Lee *et al.* 2002).

180 **Table 1:** Thermogravimetric analysis (TGA) results.

| Sample | Initial degradation temperature (°C) | Final degradation temperature (°C) | Weight loss (%) | Final residue at 900 °C (%) |
|------------------------|--------------------------------------|------------------------------------|-----------------|-----------------------------|
| PRF adhesive | 220 | 530 | 47,92 | 39,37 |
| PUR adhesive | 220 | 430 | 74,40 | 13,24 |
| <i>A. mangium</i> wood | 140 | 380 | 72,38 | 16,72 |
| PRF Glueline | 140 | 360 | 65,43 | 20,94 |
| PUR Glueline | 130 | 420 | 72,57 | 18,26 |

181
 182 Meanwhile, the weight loss of the *A. mangium* wood sample starts to occur between 30 °C
 183 up to about 130 °C, due to hydrophilic nature of wood which resulted in high moisture absorption
 184 (Crespo *et al.* 2015; Angelini *et al.* 2009). The main degradation of *A. mangium* wood occurred
 185 at 140 °C up to 380 °C and this low thermal stability performance is attributed to the degradation
 186 of lignocellulosic components of the wood (hemicellulose, cellulose and lignin) (Manya *et al.*
 187 2003). Higher lignocellulosic components caused a higher mass loss and lower initial degradation
 188 temperature (Lee *et al.* 2018; Lee *et al.* 2017). The first peak was attributed to the decomposition
 189 of hemicellulose, while the second peak can be attributed to the cellulose while degradation of
 190 lignin occurred at the wide temperature range and overlapping with the degradation of other
 191 components (Di Blasi 2008; Mészáros *et al.* 2004).

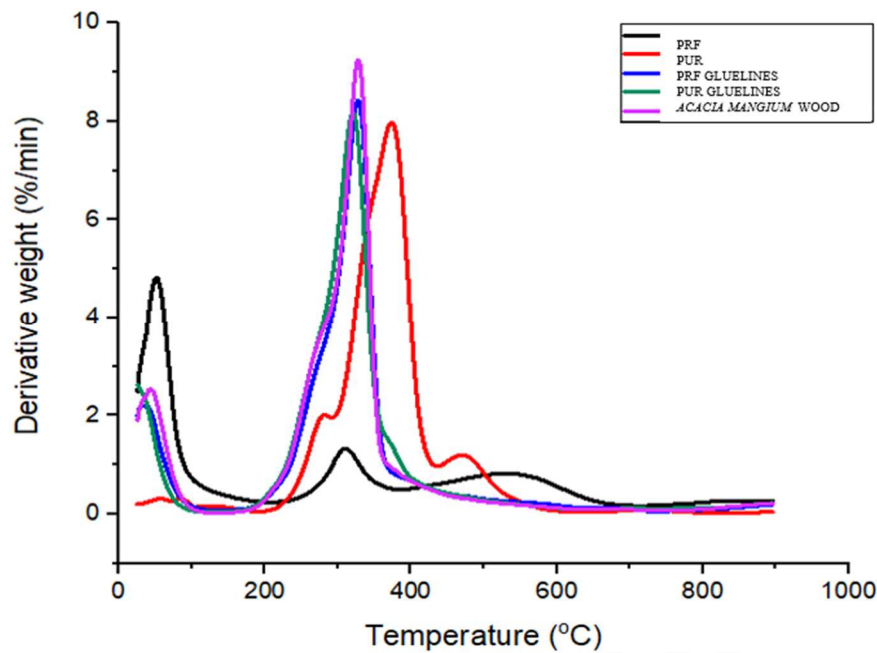
192

193 On the other hand, when both adhesives were applied on *A. mangium* wood (PRF glueline
 194 and PUR glueline), thermal degradation was expected to be similar to the degradation of pure *A.*

195 *mangium* wood. This is because only a small portion of the specimen's mass was being replaced
196 by higher thermal stability adhesive glue. Although the use of adhesive does not improve the
197 specimen's degradation temperature, the glue application slightly reduces the mass loss. PRF
198 glueline specimen was reported to have better integrity structure at temperature range up to 900
199 °C with 20,94 % of total residue compared to pure *A. mangium* wood and PUR glueline with the
200 mass residue of 16,72 % and 18,26 %, respectively. This result could be attributed to good
201 bonding properties between PRF adhesive and *A. mangium* wood compared to PUR adhesive.

202
203 Derivative thermo-gravimetric (DTG) analysis of both PRF and PUR adhesives, *A.*
204 *mangium* wood and glueline of both PRF and PUR are shown in Figure 2. DTG analysis is used
205 to study the rate of degradation of the materials up to a certain temperature (Ridzuan *et al.* 2016).
206 Three peaks were observed for all specimens which is below 100 °C, 280 °C to 380 °C and 420
207 °C to 520 °C. A low first degradation peak responsible for free water removal except for PRF
208 adhesive glue. A maximum decomposition rate at 4,83 %/min for PRF was observed due to the
209 presence of hydroxyl molecule in PRF adhesive glue (Asim *et al.* 2016). All specimens
210 demonstrate the maximum rate of weight losses in the second peak except PRF adhesive glue.
211 *A. mangium* wood showed a higher DTG value at the second peak among all the samples.
212 Meanwhile, the application of adhesive glues (PRF and PUR) on *A. mangium* wood seems to
213 reduce the rate of weight loss as part of the specimen's mass replaced by higher thermal stability
214 materials. No significance changes showed at the third region of DTG peaks for all samples.

215



216 **Figure 2:** DTG curve of PRF, PUR, PRF glue line, PUR glue line and *A. mangium* wood.

217

218 **Dynamic mechanical analysis (DMA)**

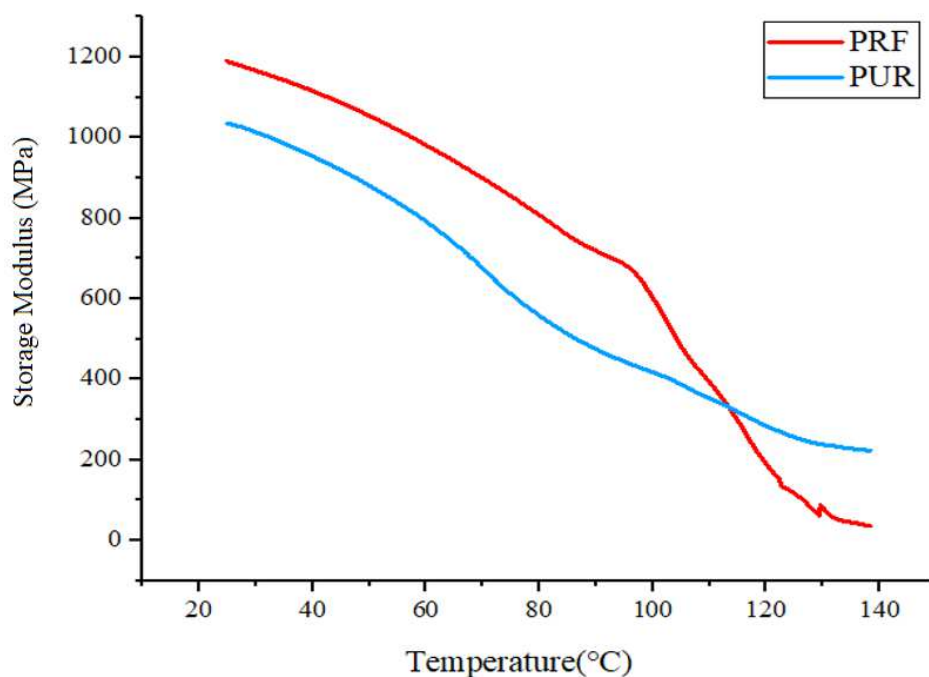
219

220 DMA is one of the most functional analysis to investigate the morphological and viscoelastic
221 properties of a material. It helps to analyse some other parameters such as primary relaxations,
222 storage or loss compliance, dynamic fragility, cross-linking density, creep compliance and
223 dynamic viscosity (Ornaghi *et al.* 2012; Pistor *et al.* 2012; Joseph *et al.* 2010, Qazvini and
224 Mohammadi 2005). It is a technique where small deformation is applied in a cyclic manner.

225

226 In this section, only the glue lines formed by PRF and PUR adhesives were tested and
227 discussed. Figure 3 illustrates the storage modulus of PRF and PUR adhesive glue lines of CLT
228 made by *A. mangium* wood. According to Saba *et al.* (2016), there are three regions found for
229 viscoelastic materials, namely glassy region, transition region and rubbery region. High storage
230 modulus value indicated the glassy region where the components are in tightly packed and drop
231 as it reached the glass transition temperature (T_g). This is because slipping of polymer chain
232 above T_g reduces its modulus and performances. As the temperature increase, the component

233 tends to increase in mobility correspond to rubbery state transition (Jawaid and Khalil 2011;
234 Hameed *et al.* 2007; Jacob *et al.* 2006). The investigation of various storage modulus with a
235 temperature of CLT was found decrease with temperature increment. At low temperature, storage
236 modulus PRF glueline is higher but close to PUR glueline, suggesting that PRF glueline has
237 better stiffness but lower mobility and flexibility (Chartoff *et al.* 2009). This finding was
238 synchronized with TGA results reported in the above section where PRF glueline has better
239 interfacial bonding between wood and PRF glue. Besides, a sudden drop of storage modulus at



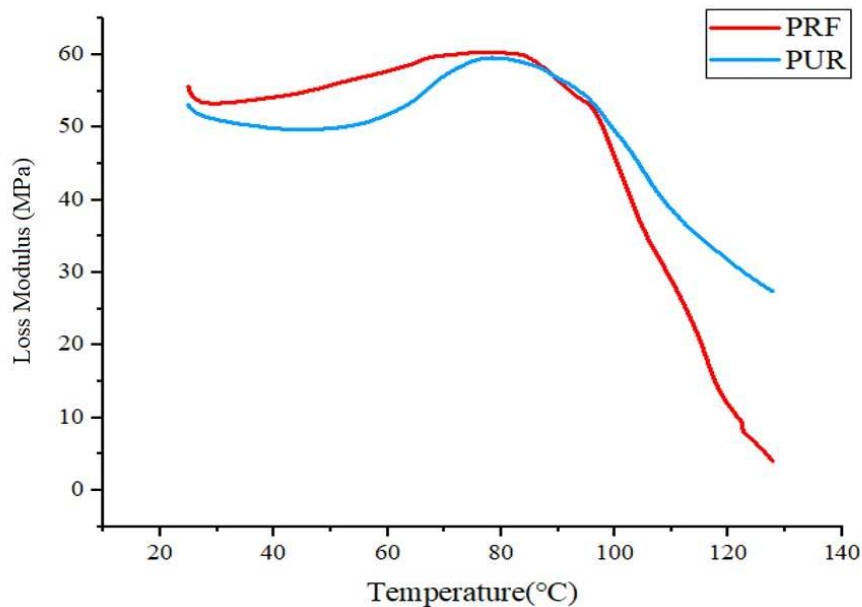
240 about 100 °C for both gluelines represents glass transition temperature, T_g zone.

241 **Figure 3:** Storage Modulus of PRF glueline and PUR glueline.

242

243 Meanwhile, the loss modulus measurement is carried out on the energy dissipation response
244 under reciprocal deformation of a material (Jawaid *et al.* 2012). Loss modulus of PRF and PUR
245 adhesive glueline of CLT made by *A. mangium* wood are illustrated in Figure 4. Both curves at
246 maximum value indicates maximum dissipation of mechanical energy at lower temperature and
247 decreased dramatically at higher temperature due to the free movement of polymer (Saba *et al.*

248 2016b). From Figure 4, both gluelines demonstrated a wide peak at 60 °C to 100 °C and the T_g
249 observed for PRF glueline is slightly lower than PUR glueline. This is because the inter-



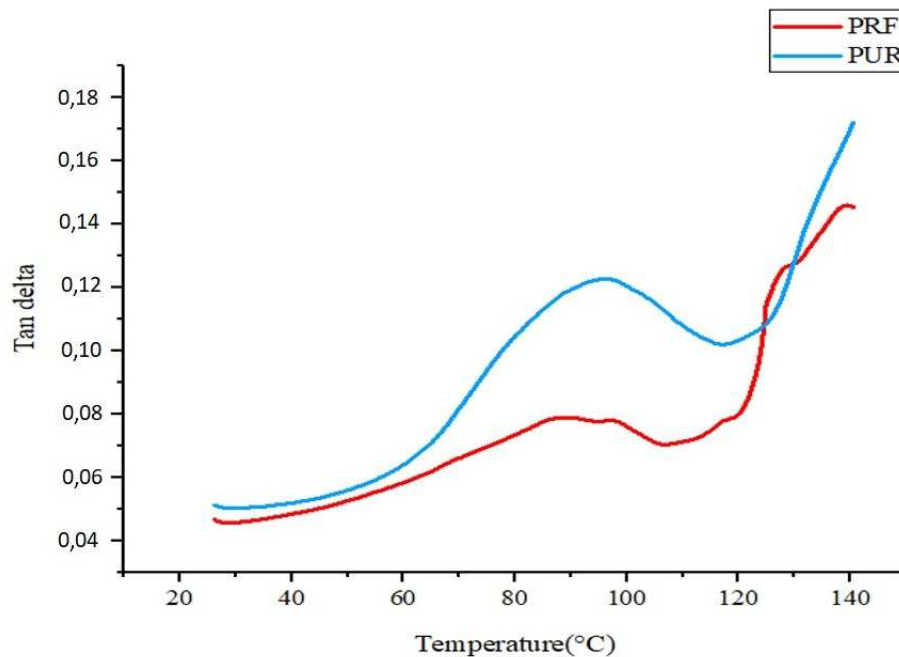
250 molecular friction in the PRF glueline was higher and increases the dissipation of energy within
251 CLT (Hameed *et al.* 2007). PRF glueline resulted in a higher loss of modulus due to the increased
252 amount of energy needed to disentangle a better interfacial bonding.

253 **Figure 4:** Loss Modulus of PRF glueline and PUR glueline.

254
255 Damping factor determines the ability of material on absorbing energy at a range of
256 temperature or frequency. Damping is important when designing advanced structural especially
257 when vibration and noise control involved. Besides, it is used to study the fatigue life and impact
258 resistance of structural materials and monitor damage (Melo and Radford 2005). Figure 5 depicts
259 the damping factor curve trend of the CLT for both types of gluelines with the temperature at
260 frequency of 1 Hz. At temperature below T_g , low $\tan \delta$ corresponds to close pack molecular
261 structure. Whilst the temperature sweep, the $\tan \delta$ increased indicate both gluelines become more
262 viscous.

263 A wide area of $\tan \delta$ peak for PUR glueline observed in this test reflecting higher dynamic
264 fragility, due to poor interfacial bonding between adhesive and wood. On the other hand, the

265 lower $\tan \delta$ peak of PRF glueline showed a good interfacial adhesion similar to the results of
266 storage modulus (Jawaid and Khalil 2011). From the $\tan \delta$ curve in Figure 5, T_g of PRF glueline
267 was also observed to be slightly lower than PUR glueline. George *et al.* (2003) evaluated two



268 commercial PRF and PUR adhesives using thermomechanical analysis (TMA) and found that
269 wood joints bonded with PUR exhibited a significant temperature-dependant creep. The finding
270 suggested that PUR is not suitable for structural application. As in this study, similar conclusion
271 can be drawn, where PUR is an inferior adhesive compared to PRF in the manufacturing of CLT.

272 **Figure 5:** Damping Factor of PRF glueline and PUR glueline.

274 CONCLUSIONS

275
276 In this study, thermogravimetric analysis was performed on both neat PRF and PUR
277 adhesives, *A. mangium* wood as well as gluelines of both PRF and PUR formed after CLT
278 fabrication process. On the other hand, dynamic mechanical analysis was conducted to
279 characterize the PRF and PUR gluelines. Generally, it was found that PRF adhesive glue was
280 more thermally stable than PUR adhesive glue, with a higher percentage of residue in TGA
281 test. Both adhesive glues start the degradation at the same temperature of 220 °C but PRF

282 adhesive showed higher degradation temperature at 530 °C at the second stage with a lower
283 percentage of weight loss of 47,92 %. As expected, *A. mangium* wood specimen has the
284 lowest thermal properties due to low thermal stability of hemicellulose. The application of
285 adhesives glue on *A. mangium* did improved the thermal stability of the wood by reducing
286 weight loss during degradation process. In comparison, PRF glueline has better thermal
287 stability compared to that PUR glueline as indicated by its higher residue at temperature up
288 to 900 °C.

289

290 In DMA, the storage modulus of PRF glueline is higher but close to PUR glueline,
291 suggesting that PRF glueline has better stiffness but lower mobility and flexibility. A sudden
292 drop of storage modulus at about 100 °C for both gluelines, indicating glass transition
293 temperature, T_g and major main chain slipping were found. The T_g of PRF glueline observed
294 from $\tan \delta$ and loss modulus curve was slightly lower than that of PUR glueline. Besides,
295 PRF glueline resulted in a higher loss of modulus due to increased amount of energy needed
296 to disentangle a better interfacial bonding. Similar trend was also found in loss modulus and
297 $\tan \delta$ curves. Based on results obtained, it can be concluded that PRF adhesive is a better
298 binding agent for *A. mangium* wood in the manufacturing of CLT as it resulted in better
299 interfacial bonding and a promising thermal performance at higher working temperature
300 compared to PUR.

301

302

ACKNOWLEDGEMENTS

303

304 This study was financially supported by the Higher Institution Centre of Excellence
305 (HiCoE) No. 6369109. The authors also would like to extend their gratitude for the facilities
306 support from HLM Wood Products Sdn. Bhd.

307

308

REFERENCES

309

310 **Angelini, L.G.; Ceccarini, L; Nassi O Di Nasso, N; Bonari, E. 2009.** Comparison of
311 *Arundo Donax* L. and *Miscanthus x Giganteus* in a long-term field experiment in central
312 Italy: analysis of productive characteristics and energy balance. *Biomass Bioenerg* 33(4):
313 635-643. <https://doi.org/10.1016/j.biombioe.2008.10.005>

314

315 **Asim, M.; Jawaid, M.; Abdan, K.; Ishak, M.R. 2016.** Effect of alkali and silane
316 treatments on mechanical and fibre-matrix bond strength of kenaf and pineapple leaf fibres. *J*
317 *Bionic Eng* 13(3): 426–35. [https://doi.org/10.1016/S1672-6529\(16\)60315-3](https://doi.org/10.1016/S1672-6529(16)60315-3)

318

319 **Asim, M.; Jawaid, M.; Nasir, M.; Saba, N. 2018.** Effect of fiber loadings and treatment
320 on dynamic mechanical, thermal and flammability properties of pineapple leaf fiber and
321 kenaf phenolic composites. *J Renew Mater* 6(4): 383–93.
322 <https://doi.org/10.7569/JRM.2017.634162>

323

324 **Aydemir, D.; Civi, B.; Alsan, M.; Can, A.; Sivrikaya, H.; Gunduz, G.; Wang, A.**
325 **2016.** Mechanical, morphological and thermal properties of nano-boron nitride treated wood
326 materials. *Maderas-Cienc Tecnol* 18(1): 19-32. [http://dx.doi.org/10.4067/S0718-](http://dx.doi.org/10.4067/S0718-221X2016005000003)
327 [221X2016005000003](http://dx.doi.org/10.4067/S0718-221X2016005000003)

327

328 **Crespo, Y.A; Naranjo, R.A; Burgos, J.C.V.; Sanchez, C.G.; Sanchez, E.M. 2015.**
329 Thermogravimetric analysis of thermal and kinetic behavior of *Acacia mangium* wood. *Wood*
330 *Fiber Sci* 47(4): 327-335. <http://wfs.swst.org/index.php/wfs/article/view/2363>

331

332 **Chartoff, R.P.; Menczel, J.D.; Dillman, S.H. 2009.** Dynamic Mechanical Analysis
333 (DMA). In *Thermal Analysis of Polymers: Fundamentals and Applications*, Menczel, J.D.;
334 Bruce Prime, R. (Eds.). John Wiley and Sons, New Jersey, USA. pp. 387–495.
335 <https://doi.org/10.1002/9780470423837.ch5>

336

337 **Di Blasi, C. 2008.** Modeling chemical and physical processes of wood and biomass
338 pyrolysis. *Prog Energy Combust Sci* 34(1): 47-90. <http://doi.org/10.1016/j.pecs.2006.12.001>

339

340 **Dieste, A.; Cabrera, M.N.; Clavijo, L.; Cassell, N. 2019.** Analysis of wood products
341 from an added value perspective: the Uruguayan forestry case. *Maderas-Cienc Tecnol* 21(3):
342 305 – 316. <http://dx.doi.org/10.4067/S0718-221X2019005000303>

343

344 **Engineering Toolbox. 2004.** Density of various wood species. Retrieved from
345 https://www.engineeringtoolbox.com/wood-density-d_40.html

346

- 347 **George, B.; Simon, C.; Properzi, M.; Pizzi, A.; Elbez, G. 2003.** Comparative creep
348 characteristics of structural glulam wood adhesives. *Holz Roh Werkst* 61(1): 79-80.
349 <https://doi.org/10.1007/s00107-002-0348-3>
- 350 **Hameed, N.; Sreekumar, P.A.; Francis, B.; Yang, W.; Thomas, S. 2007.**
351 Morphology, dynamic mechanical and thermal studies on poly (styrene-co-acrylonitrile)
352 modified epoxy resin/glass fibre composites. *Compos Part A Appl Sci Manuf* 38(12): 2422-
353 2432. <https://doi.org/10.1016/j.compositesa.2007.08.009>
354
- 355 **Jacob, M.; Francis, B.; Varughese, K.; Thomas, S. 2006.** The effect of silane coupling
356 agents on the viscoelastic properties of rubber biocomposites. *Macromol Mater Eng* 291(9):
357 1119-1126. <https://doi.org/10.1002/mame.200600171>
358
- 359 **Jawaid, M.; Abdul Khalil, H.P.S.; Alattas, O. 2012.** Woven hybrid biocomposites:
360 dynamic mechanical and thermal properties. *Compos Part A Appl Sci Manuf* 43(2): 288-
361 293. <https://doi.org/10.1016/j.compositesa.2011.11.001>
362
- 363 **Jawaid, M.; Abdul Khalil, H.P.S. 2011.** Effect of layering pattern on the dynamic
364 mechanical properties and thermal degradation of oil palm-jute fibers reinforced epoxy
365 hybrid composite. *BioResources* 6(3): 2309-2322.
366 [https://ojs.cnr.ncsu.edu/index.php/BioRes/article/view/BioRes_06_3_2309_Jawaid_A_Lay](https://ojs.cnr.ncsu.edu/index.php/BioRes/article/view/BioRes_06_3_2309_Jawaid_A_Layering_Pattern_DMA_Epoxy_Hybrid_Composites)
367 [ering_Pattern_DMA_Epoxy_Hybrid_Composites](https://ojs.cnr.ncsu.edu/index.php/BioRes/article/view/BioRes_06_3_2309_Jawaid_A_Layering_Pattern_DMA_Epoxy_Hybrid_Composites)
368
- 369 **Johar, N.; Ahmad, I.; Dufresne, A. 2012.** Extraction, preparation and characterization
370 of cellulose fibres and nanocrystals from rice husk. *Ind Crops Prod* 37(1): 93-99.
371 <https://doi.org/10.1016/j.indcrop.2011.12.016>
372
- 373 **Joseph, S.; Appukuttan, S.P.; Kenny, J.M.; Puglia, D.; Thomas, S.; Joseph, K. 2010.**
374 Dynamic Mechanical Properties of oil palm microfibril-reinforced natural rubber
375 composites. *J Appl Polym Sci* 117(3): 1298-1308. <https://doi.org/10.1002/app.30960>
376
- 377 **Kasim, A.; Omar, W.S.A.W.; Razak, N.H.A.; Musa, N.L.W.; Halim, R.A.;
378 Mohamed, S.R. 2014.** *Proceedings of the International Conference on Science, Technology
379 and Social Sciences (ICSTSS) 2012.* Springer Singapore, Singapore.
380
- 381 **Lee, C.H.; Sapuan, S.M.; Hassan, M.R. 2018.** Thermal analysis of kenaf fiber
382 reinforced floreon biocomposites with magnesium hydroxide flame retardant filler. *Polym*

383 *Compos* 39(3): 869-875. <https://doi.org/10.1002/pc.24010>

384

385 **Lee, C.H.; Sapuan, S.M.; Hassan, M.R. 2017.** Mechanical and thermal properties of
386 kenaf fiber reinforced polypropylene/magnesium hydroxide composites. *J Eng Fiber Fabr*
387 12(2): 50-58. <https://doi.org/10.1177%2F155892501701200206>

388

389 **Lee, S.H.; Teramoto, Y.; Shiraishi, N. 2002.** Biodegradable polyurethane foam from
390 liquefied waste paper and its thermal stability, biodegradability, and genotoxicity. *J Appl*
391 *Polym Sci* 83(7): 1482-1489. <https://doi.org/10.1002/app.10039>

392

393 **Lim, S.C.; Gan, K.S.; Choo, K.T. 2003.** The characteristics, properties and uses of
394 plantation timbers; rubberwood and Acacia mangium. *Timber Technology Bulletin* 26: 1-10.
395 <https://info.frim.gov.my/infocenter/booksonline/ttb/TTBno26.pdf>

396 **Liu, J; Chen, R.Q; Xu, Y.Z.; Wang, C.P.; Chu, F.X. 2017.** Resorcinol in high solid
397 phenol–formaldehyde resins for foams production. *J Appl Polym Sci* 134(22): 44881.
398 <https://doi.org/10.1002/app.44881>

399

400 **Manya, J.J.; Velo, E.; Puigjaner, L. 2003.** Kinetics of biomass pyrolysis: a
401 reformulated three-parallel-reactions model. *Ind Eng Chem Res* 42(3): 434-441.
402 <https://doi.org/10.1021/ie020218p>

403

404 **Melo, J.D.; Radford, D.W. 2005.** Time and temperature dependence of the
405 viscoelastic properties of cfrp by dynamic mechanical analysis. *Compos Struct* 70(2): 240-
406 253. <https://doi.org/10.1016/j.compstruct.2004.08.025>

407

408 **Mészáros, E.; Várhegyi, G.; Jakab, E.; Marosvölgyi, B. 2004.** Thermogravimetric
409 and reaction kinetic analysis of biomass samples from an energy plantation. *Energ*
410 *Fuel* 18(2): 497–507. <https://doi.org/10.1021/ef034030+>

411

412 **Miranda, I.M.; Almeida, H.; Pereira, H. 2007.** Influence of provenance, subspecies,
413 and site on wood density in *Eucalyptus globulus* Labill. *Wood Fiber Sci* 33(1): 9–15.
414 <https://wfs.swst.org/index.php/wfs/article/view/66>

415

416 **Nadirah, W.O.; Jawaid, M.; Al Masri, A.A.; Abdul Khalil, H.P.S.; Suhaily, S.S.;**
417 **Mohamed, A.R. 2012.** Cell wall morphology, chemical and thermal analysis of cultivated
417 pineapple leaf fibres for industrial applications. *J Polym Environ* 20(2): 404-411.

418 <https://doi.org/10.1007/s10924-011-0380-7>

419

420 **Nordahlia, A.S.; Hamdan, H.; Anwar, U.M.K. 2013.** Wood properties of selected
421 plantation species: *Khaya ivorensis* (african mahogany), *Azadirachta excelsa* (sentang),
422 *Endospermum malaccense* (sesendok) and *Acacia mangium*. *Timber Technology Bulletin* 51:
423 1-4. <https://info.frim.gov.my/infocenter/booksonline/ttb/TTB51.pdf>

424

425 **Norwahyuni, M.Y.; Tahir, P.M.; Roseley, A.S.M.; Lee, S.H.; Halip, J.A.; James,**
426 **R.M.S.; Ashaari, Z. 2019a.** Bond integrity of cross laminated timber from *Acacia mangium*
427 wood as affected by adhesive types, pressing pressures and loading direction. *Int J Adhes*
428 *Adhes* 94: 24-28. <https://doi.org/10.1016/j.ijadhadh.2019.05.010>

429

430 **Norwahyuni, M.Y.; Tahir, P.M.; Lee, S.H.; Khan, M.A.; James, R.M.S. 2019b.**
431 Mechanical and physical properties of Cross-Laminated Timber made from *Acacia mangium*
432 wood as function of adhesive types. *J Wood Sci* 65(1): 20. [https://doi.org/10.1186/s10086-](https://doi.org/10.1186/s10086-019-1799-z)
433 [019-1799-z](https://doi.org/10.1186/s10086-019-1799-z)

434

435 **Nugroho, W.D.; Marsoem, S.N.; Yasue, K.; Fujiwara, T.; Nakajima, T.; Hayakawa,**
436 **M.; Nakaba, S.; Yamagishi, Y.; Jin, H.; Kubo, T.; Funada, R. 2012.** Radial variations in
437 the anatomical characteristics and density of the wood of acacia mangium of five different
438 provenances in Indonesia. *J Wood Sci* 58(3): 185-194. [https://doi.org/10.1007/s10086-011-](https://doi.org/10.1007/s10086-011-1236-4)
439 [1236-4](https://doi.org/10.1007/s10086-011-1236-4)

440

441 **Ornaghi, H.L.; Pistor, V.; Zattera, A.J. 2012.** Effect of the epoxy cyclohexyl
442 polyhedral oligomeric silsesquioxane content on the dynamic fragility of an epoxy resin. *J*
443 *Non Cryst Solids* 358(2): 427-432. <https://doi.org/10.1016/j.jnoncrsol.2011.10.014>

444

445 **Pistor, V.; Ornaghi, F.G.; Ornaghi, H.L.; Zattera, A.J. 2012.** Dynamic mechanical
446 characterization of epoxy/epoxycyclohexyl-POSS nanocomposites. *J Mater Sci Eng A* 532:
447 339-345. <https://doi.org/10.1016/j.msea.2011.10.100>

448

449 **Qazvini, N.T.; Mohammadi, N. 2005.** Dynamic Mechanical Analysis of segmental
450 relaxation in unsaturated polyester resin networks: effect of styrene content. *Polymer* 46(21):
451 9088-9096. <https://doi.org/10.1016/j.polymer.2005.06.118>

452

453 **Ridzuan, M.J.M.; Majid, M.A.; Afendi, M.; Mazlee, M.N.; Gibson, A.G. 2016.**
454 Thermal behaviour and dynamic mechanical analysis of pennisetum purpureum/glass-
455 reinforced epoxy hybrid composites. *Compos Struct* 152: 850-859.
456 <https://doi.org/10.1016/j.compstruct.2016.06.026>

457
458 **Richter, K.; Pizzi, A.; Despres. A. 2006.** Thermal stability of structural one-component
459 polyurethane adhesives for wood-structure-property relationship. *J Appl Sci* 102(6): 5698–
460 5707. <https://doi.org/10.1002/app.25084>

461
462 **Saba, N.; Jawaid, M.; Alothman, O.Y.; Paridah. M. T. 2016a.** A review on dynamic
463 mechanical properties of natural fibre reinforced polymer composites. *Constr Builds Mater*
464 106(1): 149-159. <https://doi.org/10.1016/j.conbuildmat.2015.12.075>

465 **Saba, N.; Paridah, M.T.; Abdan, K.; Ibrahim, N.A. 2016b.** Dynamic Mechanical
466 Properties of oil palm nano filler/kenaf/epoxy hybrid nanocomposites. *Constr Builds*
467 *Mater* 124: 133-138. <https://doi.org/10.1016/j.conbuildmat.2016.07.059>

468
469 **Sanyang, M.L.; Sapuan, S.M.; Jawaid, M.; Ishak, M.R.; Sahari, J. 2015.** Effect of
470 plasticizer type and concentration on tensile, thermal and barrier properties of biodegradable
471 films based on sugar palm (*Arenga pinnata*) starch. *Polymer* 7(6): 1106-1124.
472 <https://doi.org/10.3390/polym7061106>

473
474 **Shukla, S.R. 2019.** Evaluation of dimensional stability, surface roughness, colour,
475 flexural properties and decay resistance of thermally modified *Acacia*
476 *auriculiformis*. *Maderas-Cienc Tecnol* 21(4): 433-446. [http://dx.doi.org/10.4067/S0718-](http://dx.doi.org/10.4067/S0718-221X2019005000401)
477 [221X2019005000401](http://dx.doi.org/10.4067/S0718-221X2019005000401)

478
479 **Sutton, A.; Black, D.; Walker, P. 2011.** Cross-Laminated Timber: an introduction to
480 low-impact building materials. IHS BRE Press, Watford, UK.

481
482 **Van De Kuilen, J.W.G.; Ceccotti, A.; Xia, Z.; He, M. 2011.** Very tall wooden
483 buildings with cross laminated timber selection and/or peer-review under
484 responsibility. *Procedia Eng* 14: 1621-1628. <https://doi.org/10.1016/j.proeng.2011.07.204>

485
486 **Wang, Z.; Zhou, J.; Dong, W.; Yao, Y.; Gong, M. 2018.** Influence of technical
487 characteristics on the rolling shear properties of cross laminated timber by modified planar

488 shear tests. *Maderas-Cienc Tecnol* 20(3): 469-478. <http://dx.doi.org/10.4067/S0718-221X2018005031601>
489
490

Accepted manuscript